Irradiation-induced microstructure of tungsten and helium embrittlement

S.L. Dudarev and M.R. Gilbert

EURATOM/CCFE Fusion Association, Culham Centre for Fusion Energy, Oxfordshire OX14 3DB

A.E. Sand and K. Nordlund

Association EURATOM-Tekes, Department of Physics, University of Helsinki, Finland

Outline

- Neutron-induced transmutation effects.
- Microstructural evolution: a simple model for He embrittlement.
- Microstructural evolution: radiation defect production, defect clustering scaling laws.

Acknowledgements

Work at CCFE was funded by the RCUK Energy Programme under grant EP/I501045 and by the European Communities under the contract of association between EURATOM and CCFE. The views and opinions expressed herein do not necessarily reflect those of the European Commission.

CCFE is the fusion research arm of the United Kingdom Atomic Energy Authority

An integrated modelling approach to fusion power plant design

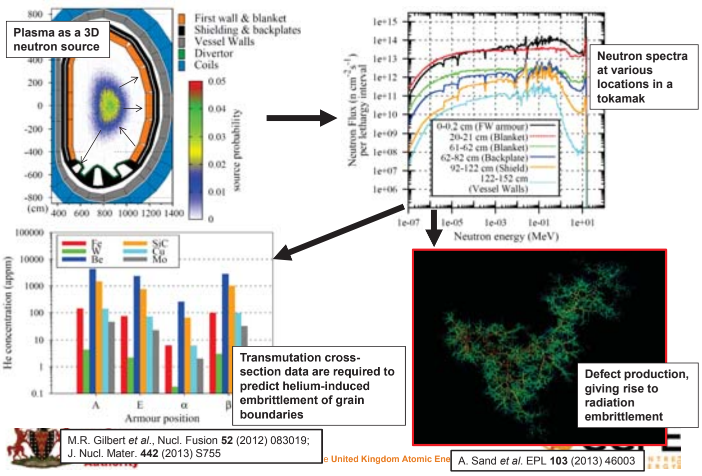

M.R. Gilbert *et al.*, Nucl. Fusion **52** (2012) 083019; J. Nucl. Mater. **442** (2013) S755

A. Sand *et al.* EPL **103** (2013) 46003

CCFE is the fusion research arm of the United Kingdom Atomic Energy Authority

Effect of giant resonances on neutron spectra in tungsten W

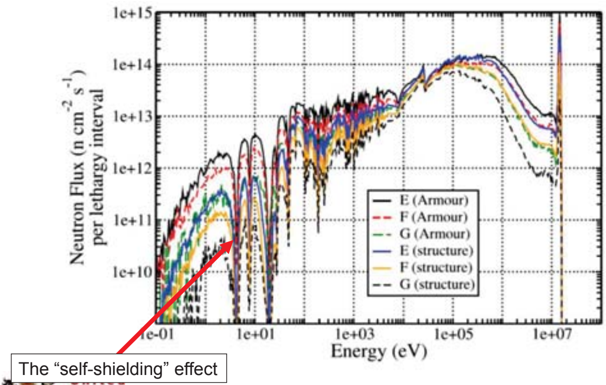

M R Gilbert and J-C Sublet, Nucl. Fusion **51** (2011) 043005

CCFE is the fusion research arm of the United Kingdom Atomic Energy Authority

Transmutations due to exposure to neutrons W

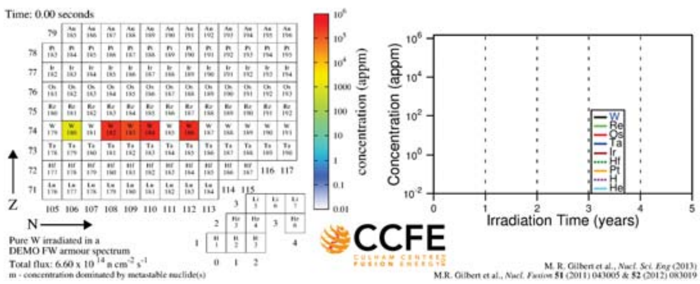

M. R. Gilbert et al., Nucl. Sci. Eng (2013)
M.R. Gilbert et al., Nucl. Fusion **51** (2011) 043005 & **52** (2012) 083019

Nuclear reactions with incident neutrons give rise to transmutations. The animated diagram above shows how the initially pure natural tungsten, exposed to neutrons with the spectrum characteristic of a DEMO fusion reactor, transforms into other elements, including helium and hydrogen. Accumulation of helium gives rise to the degradation of properties of the material and specifically to grain boundary embrittlement.

CCFE is the fusion research arm of the United Kingdom Atomic Energy Authority

The role of resonance reactions W

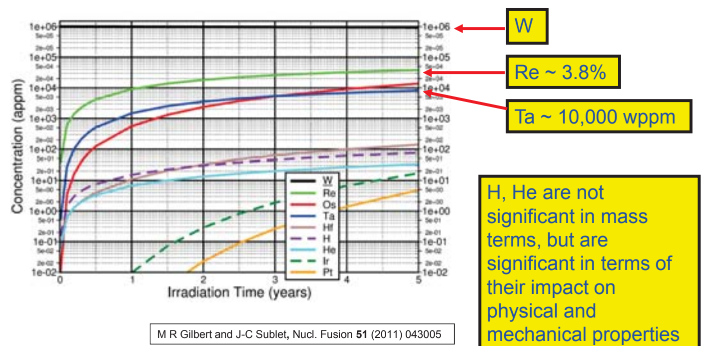

M R Gilbert and J-C Sublet, Nucl. Fusion **51** (2011) 043005

CCFE is the fusion research arm of the United Kingdom Atomic Energy Authority

Fe

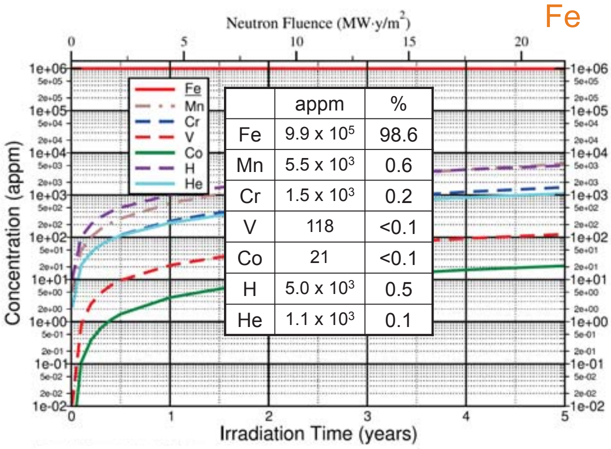

	appm	%
Fe	9.9×10^5	98.6
Mn	5.5×10^3	0.6
Cr	1.5×10^3	0.2
V	118	<0.1
Co	21	<0.1
H	5.0×10^3	0.5
He	1.1×10^3	0.1

M R Gilbert and J-C Sublet, Nucl. Fusion **51** (2011) 043005

CCFE is the fusion research arm of the United Kingdom Atomic Energy Authority

Accumulation of helium and hydrogen

- He and H concentrations after five years exposure in DEMO (in appm):

	Fe	Fe-9%Cr	W	SiC	Be	Cu
He	1091	1064	33	11253	32406	1062
H	5006	4918	79	4249	748	7332

- W-alloy results:

	W	W-30%Re	W-30%Ta	W-30%Ti	W-30%V
He	33	29	32	298	132
H	79	86	84	951	832

M R Gilbert and J-C Sublet, Nucl. Fusion **51** (2011) 043005

CCFE is the fusion research arm of the United Kingdom Atomic Energy Authority

W

Transmutation effects in ITER

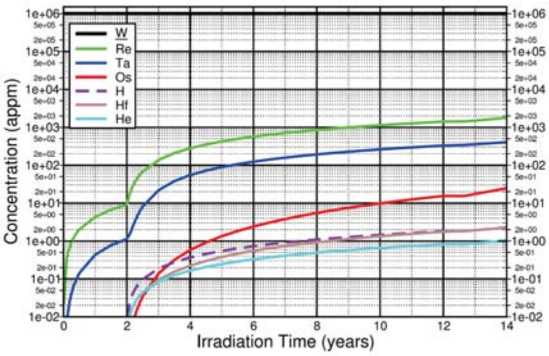

M R Gilbert and J-C Sublet, Nucl. Fusion **51** (2011) 043005

Transmutation and irradiation-induced embrittlement

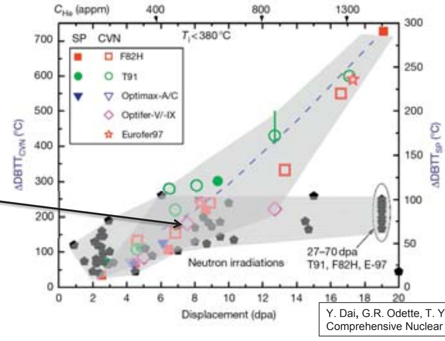

Y. Dai, G.R. Odette, T. Yamamoto, in: Comprehensive Nuclear Materials (2012)

Irradiation tests performed using spallation neutron source SINQ show that helium accumulation in steels at levels exceeding ~500 appm results in significant helium-induced grain boundary embrittlement. Helium embrittlement cannot be mitigated by optimizing the power plant operating conditions.

A helium embrittlement model

Helium atoms, produced homogeneously in the bulk of the material, migrate to grain boundaries or form bubbles inside the grains.

The total number of helium atoms inside the grain is

$$N_{He} \approx \frac{4}{3}\pi R^3 n G_{He}$$

This estimate assumes that the grain is a sphere, G_{He} is the total number of He atoms (in units of He atoms per atom of the material, e.g. appm).

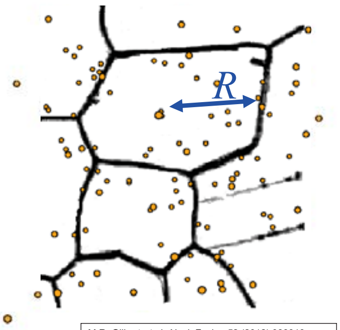

M.R. Gilbert *et al.*, Nucl. Fusion **52** (2012) 083019, Journal of Nuclear Materials **442** (2013) S755–S760.

A helium embrittlement model

If all the helium atoms produced in the interior of the grain migrate to grain boundaries, then the grain boundary density ν_{He} of He atoms (per unit grain boundary area) satisfies equation

$$4\pi R^2 \nu_{He} = \frac{4}{3}\pi R^3 n G_{He}$$

$$\nu_{He} = \frac{R}{3} n G_{He}$$

The grain boundary surface helium density scales linearly with the grain size (assuming no retention of He in the grain interior).

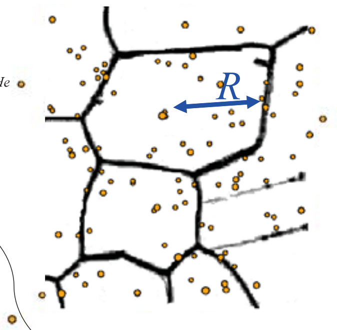

$n = 8.5 \cdot 10^{22}\ cm^{-3}$ (Fe)

A helium embrittlement model

Grain structure of the material destabilizes if the stored energy associated with helium acumulated at boundaries equals the energy of a configuration where all the grain boundaries are treated as free surfaces. The critical helium concentration

$$E_{He}\nu_{He} \cong 2\varepsilon_{surface}$$

Here E_{He} is the energy associated with embedding of a free He atom into the lattice. The estimated critical helium concentrations depend weakly on the environmental dependence of this parameter.

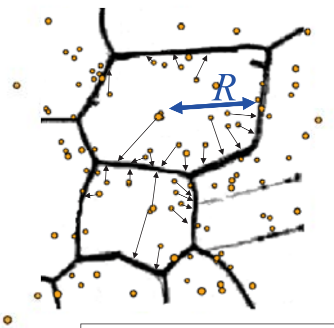

M.R. Gilbert *et al.*, Nucl. Fusion **52** (2012) 083019, Journal of Nuclear Materials **442** (2013) S755–S760.

A helium embrittlement model

Estimated critical bulk helium concentrations

Element	Critical He concentration at GBs (cm^{-2}) $\nu_c \cong \frac{2\varepsilon_{surface}}{E_{He}}$	Grain boundary radius R (μm)	Critical bulk He content G_{He} (appm)	Time to reach critical He concentration (power-plant first-wall, years)
Fe	$6.6 \cdot 10^{14}$	0.5	396	1½-2
V	$10.3 \cdot 10^{14}$	0.5	618	8-9
Cr	$5.7 \cdot 10^{14}$	0.5	342	2-2½
Mo	$7.1 \cdot 10^{14}$	0.5	426	6-7
Nb	$10.5 \cdot 10^{14}$	0.5	630	8-9
Ta	$10.7 \cdot 10^{14}$	0.5	642	86
W	**$7.6 \cdot 10^{14}$**	0.5	456	71
Be	$5.3 \cdot 10^{14}$	0.5	318	<0.1
SiC	$30 \cdot 10^{14}$	0.5	1806	~1

$n = 10^{23}\ cm^{-3}$ (estimate)

M.R. Gilbert *et al.*, Nucl. Fusion **52** (2012) 083019, Journal of Nuclear Materials **442** (2013) S755–S760.

A helium embrittlement model

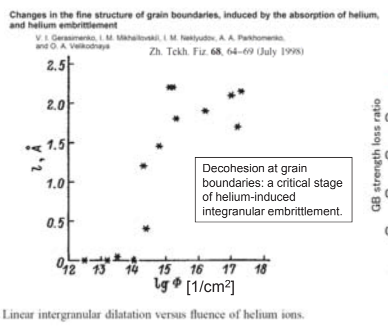

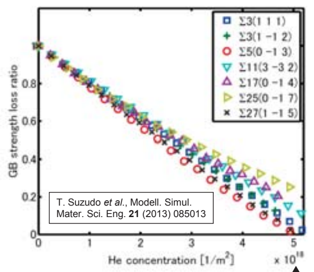

$5 \cdot 10^{14}$ cm^{-2}

The relatively simple criterion for grain boundary decohesion agrees with *ab initio* calculations showing the reduction of grain boundary strength due to the accumulation of helium (Suzudo *et al.*, 2013). It also agrees with experimental observations exhibiting grain boundary decohesion (Gerasimenko *et al.*, 1998)

Radiation damage generation in tungsten

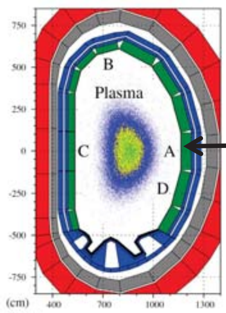

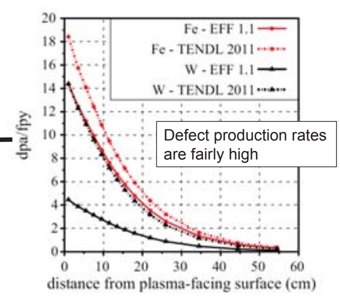

There are various uncertainties associated with defect production estimates, for example the defect production rates are sensitive to the neutron scattering cross-section values, and defect production energy thresholds. Furthermore, even an accurate calculation of NRT dpa values does not provide the information required for the assessment of the effect of radiation damage on properties of materials.

M.R. Gilbert *et al.*, Journal of Nuclear Materials **442** (2013) S755–S760.

Collision cascades in tungsten

The maximum cascade energy is (a non-relativistic equation assuming head-on elastic neutron-atom impact)

$$E_{\max} \approx \frac{4mM}{(m+M)^2} E_n \approx 300\ \text{keV};$$

$$E_n = 14.1\ \text{MeV}$$

A 150 keV cascade in tungsten: first MD simulations of “fusion” cascades

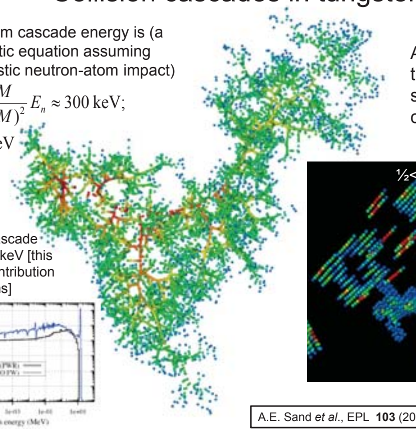

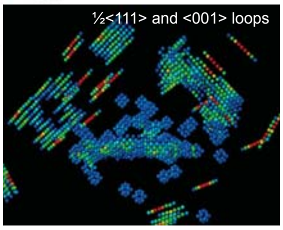

The average cascade energy is ~150 keV [this neglects the contribution of (n,γ) reactions]

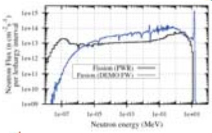

A.E. Sand *et al.*, EPL **103** (2013) 46003

A surprising discovery: iron

It has been found recently that in iron high energy cascades do not break up into sub-cascades even at the cascade energy of 500 keV.

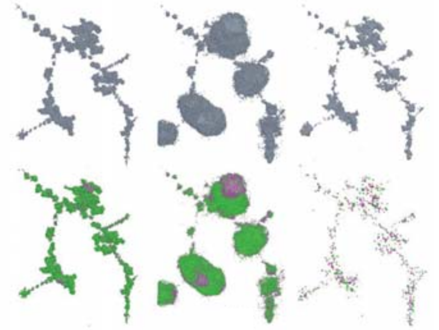

E. Zarkadoula, M.T. Dove, K. Trachenko, S.L. Daraszewicz, D.M. Duffy, M. Seaton, I.T. Todorov, and K. Nordlund, J. Phys. Condens. Matter **25** (2013) 125402

Defect production in tungsten

A.E. Sand et al., EPL **103** (2013) 46003

- The trajectories of atoms with K.E. > 10 eV show a high degree of branching – cascades are fractal

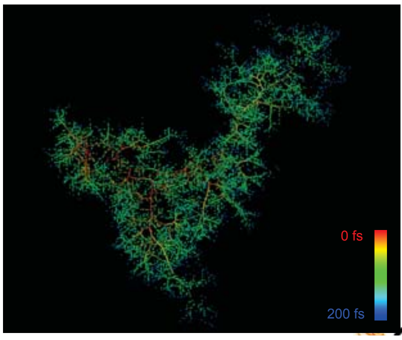

[Fractal nature of cascades: J.C. Moreno Marin, U. Conrad, H.M. Urbassek, A. Gras-Marti, Nucl. Instr. Meth. B 48 (1990) 404-407]

Defect production in tungsten

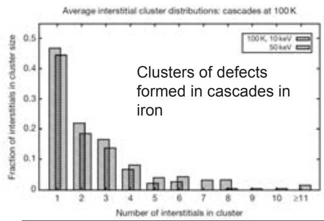

R.E. Stoller (2012) in: Comprehensive Nuclear Materials

Prior to 1991 it was assumed that defects were produced as Frenkel pairs (individual vacancies and self-interstitials). C.H. Woo and B.N. Singh (1991) noted that clustering of defects in cascades may have a significant effect on radiation-induced microstructure.

T. Diaz de la Rubia, M.W. Guinan, PRL **66** (1991) 2766; C.H. Woo, B.N. Singh, Phil. Mag. **65** (1992) 889-912

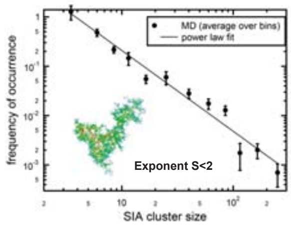

Distribution of defect cluster sizes follows a power law

$$F(n) = \frac{A}{n^S}; n < n^* \approx 600$$

$$A \approx 7.45\,; S = 1.63$$

A.E. Sand et al., EPL **103** (2013) 46003

The power law of defect clustering

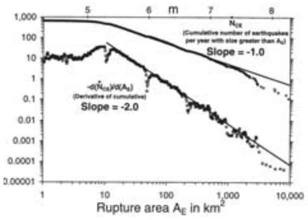

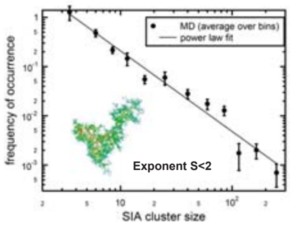

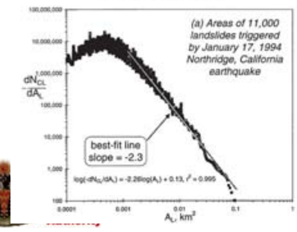

Power-law type distributions of frequencies of events are not uncommon. They often describe phenomena, the theoretical treatment of which is not immediately evident.

Treatment of defect clustering in cascades has so far remained elusive, and the emergence of a power law statistics is perhaps not surprising.

The significance of large clusters

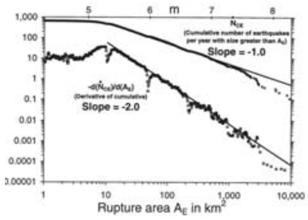

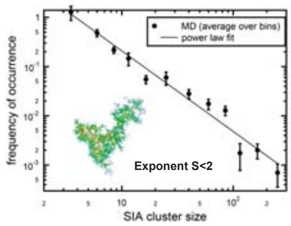

Total number of defects produced

$$N = \int_1^{n^*} nF(n)dn \approx \frac{A}{2-S}(n^*)^{2-S}$$

Large clusters are rare BUT if they form then they contain the majority of defects. Large rarely occurring defects dominate microstructural evolution.

Distribution of defect cluster sizes follows a power law

$$F(n) = \frac{A}{n^S}; n < n^* \approx 600$$

$$A \approx 7.45\,; S = 1.63 < 2!$$

A.E. Sand *et al.*, EPL **103** (2013) 46003

Driving force for defect clustering in tungsten

Agglomeration of point defects gives rise to the formation of interstitial dislocation loops (=clusters of self-interstitial atoms) or voids/vacancy dislocation loops (= clusters of vacancies). In both cases, energy minimization drives clustering of defects.

Green dashed line shows the total energy of formation of N individual self-interstitial atom defects.

Purple dashed line shows the formation energy of N individual vacancies.

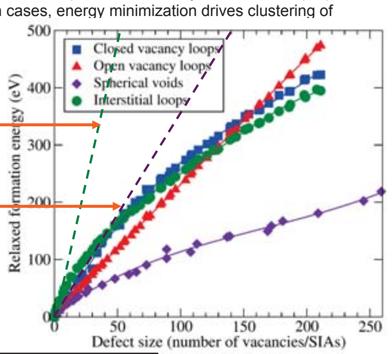

M.R. Gilbert *et al.*, J. Phys. Cond. Matter **20** (2008) 345214

Defect clusters in tungsten

Loops with both ½<111> and <001> Burgers vectors have been found in cascade simulations. Loops with two different Burgers vectors have different properties and contribute differently to microstructural evolution. In tungsten that, unlike iron, is elastically isotropic, the occurrence of the <001> loops is not related to elastic anisotropy.

A.E. Sand *et al.*, EPL **103** (2013) 46003

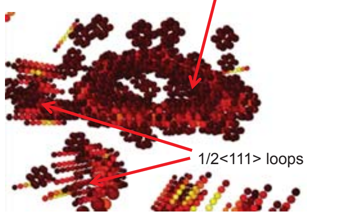

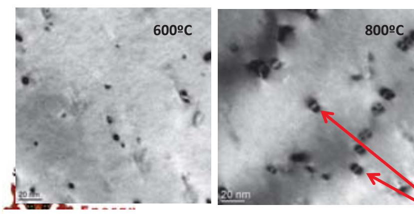

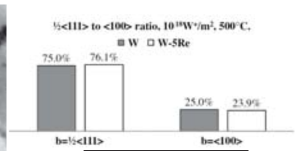

X.Yi, M.L. Jenkins et al., Philos. Mag. **93** (2013) 1715

Microstructure of W irradiated to 1 dpa, note the temperature effect

Dislocation loops

New interatomic potentials for tungsten

Reliability of cascade simulations critically depends on (i) the quality of interatomic potentials used and (ii) the treatment of dissipation and energy losses.

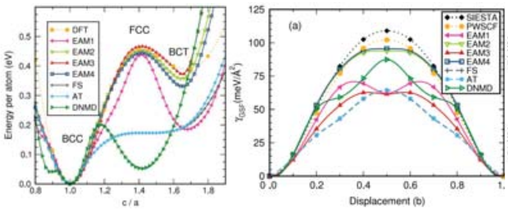

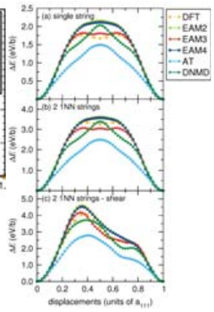

A small family of three semi-empirical EAM-type interatomic potentials for tungsten have now been developed. EAM2 and EAM4 potentials appear to provide fairly good match to DFT and experimental data [especially on dislocations].

M.-C. Marinica *et al.*, J. Phys. Cond. Matter **25** (2013) 395502

Summary

- Neutron-induced transmutation effects can be quantified, for the tungsten case they are fairly sensitive to the neutron spectrum.
- Estimates of He embrittlement effects can be given in relatively simple terms, accurate predictions require detailed modelling of microstructure.
- Damage cannot be characterized by a single “dpa” parameter, information on defect clustering in cascades, their interaction and subsequent evolution is required.
- New insight: analysis of scaling laws suggest that rare large events probably dominate microstructural evolution. Implications for damage accumulation, helium and hydrogen retention etc.